



Hossain, K., Sabapathy, T., Jusoh, M., Soh, P. J., Ahmad, R. B., Jais, M. I., Osman, M. N. and Abbasi, Q. H. (2022) A frequency-reconfigurable microstrip antenna with constant dipole-like radiation patterns using single bias, triple varactor tuning with reduced complexity. *Wireless Personal Communications*, 123(2), pp. 1003-1024.

(doi: [10.1007/s11277-021-09167-8](https://doi.org/10.1007/s11277-021-09167-8))

This is the Author Accepted Manuscript.

There may be differences between this version and the published version. You are advised to consult the publisher's version if you wish to cite from it.

<https://eprints.gla.ac.uk/253165/>

Deposited on: 28 September 2021

# A Frequency-Reconfigurable Microstrip Antenna with Constant Dipole-Like Radiation Patterns using Single Bias, Triple Varactor Tuning with Reduced Complexity

Kabir Hossain<sup>1,2</sup> . Thennarasan Sabapathy<sup>1,2</sup> . Muzammil Jusoh<sup>1,2</sup> . Ping Jack Soh<sup>2,3</sup> .

R. Badlishah Ahmad<sup>2,4</sup> . Mohd Ilman Jais<sup>2,4</sup> . Mohamed Nasrun Osman<sup>1,2</sup> . Qammer H. Abbasi<sup>5</sup>

## Abstract

This work proposes a novel frequency-reconfigurable circular patch antenna incorporated with a rectangular slot and a narrow slot capable of producing constant dipole-like radiation patterns. The antenna compactness is achieved with the integration of the rectangular slot defected ground structure (DGS) on the ground. The proposed antenna is able to perform continuous frequency tuning between 1.91 GHz and 2.77 GHz with a frequency ratio of 1.5:1, in addition to stable dipole-like radiation patterns. The resonant frequency of the antenna is controlled by tuning a simple DC biasing network that consists of three RF varactor diodes located on the narrow slot DGS. Implementing the DC biasing network at the narrow slot DGS while maintaining the large slot DGS helps the antenna miniaturization and maintains the constant dipole-like radiation pattern over all frequency tuning range. The results are validated via simulations and experimental validations in terms of reflection coefficients and the radiation patterns. Measurements indicated that an impedance bandwidth of 85 MHz is featured for each tuned frequency band, with dipole-like patterns and an average gain of 1.57 dBi.

**Keywords** Reconfigurable antenna, antenna and propagation, defected ground structure (DGS), slot antenna.

## 1. Introduction

Reconfigurable antenna is proving essential for future wireless and communication systems due to its capability to tune and control in terms of frequency, polarization and/or radiation pattern. Frequency reconfigurable antenna is capable of operating at multi-frequency bands with the aid of single hardware which is cost-effective, compact size and flexible [1–3]. In the cognitive radio (CR) application for channel sensing, the reconfigurable antenna is one of the most efficient solutions [4]–[5]. In literature, the four major techniques are proposed to achieve the reconfigurability termed as electrical, optical, physical and material tuning [1, 6]. The switching operations in the reconfigurable antennas can be achieved using PIN diodes [2, 3, 7–9], varactor diodes [10–14] and RF-MEMS [15–17]. The switching assist in altering their surface currents and which allows the electrical reconfigurability of

antennas. The switches alter the electric properties by changing the effective lengths of the antenna [3]. It is evident that the use of a greater number of PIN diodes enable reconfigurability of the antenna to multiple frequency bands. However, if the forward bias is applied to PIN diodes, it requires significant amount of current to overcome the ohmic resistance. It leads to RF power loss, which results in significant decrease of antenna efficiency [10]. However, the varactor diodes in contrast to PIN diode allow frequency tuning throughout a wider frequency range. This is achieved by modulating its capacitance and isolation loss when applying reverse bias voltage [18]. However, such configuration does not typically allow tuning with large frequency ratios [10, 13, 14].

Efforts in compacting the size of microstrip patch antennas have been on the rise in the recent years due to such requirement in wireless communication devices [19]. Several

---

✉ Thennarasan Sabapathy  
thennarasan@unimap.edu.my

1. Advanced Communication Engineering (ACE), Centre of Excellence, Universiti Malaysia Perlis (UniMAP), Perlis, Malaysia.  
2. Faculty of Electronic Engineering Technology, Universiti Malaysia Perlis (UniMAP), Perlis, Malaysia  
3. Centre for Wireless Communications (CWC), University of Oulu, P.O. Box 4500, 90014 University of Oulu, Finland  
4. Centre of Excellence Advance Computing (AdvComp), Universiti Malaysia Perlis (UniMAP), Perlis, Malaysia  
5. James Watt School of Engineering, University of Glasgow, United Kingdom

methods are proposed in literature to reduce antennas size, defected ground structure (DGS) and defected microstrip structure (DMS) [20, 21]. Introduction of a DGS structure into the ground plane of an antenna results into variation of parameters such as capacitance and inductance, which alters the path of current flow and thus results in reduction of its size [19]. Several antennas have been miniaturized in size using different DGS structures on the ground plane, e.g.; hexagonal [22, 23], slot-line [24], U- and I-shape slots [25], rectangular slot [26], and etc. In [26], a rectangular slot DGS was incorporated for size compactness and varactor diodes were integrated into the slot to tune the antenna from 4.65 GHz to 6.18 GHz. Similarly, a hexagonal shaped DGS was used in [20] to miniaturize the antenna and varactor diodes were used to enable frequency reconfigurability from 1.41 to 2.26 GHz. One of the key issues found in existing microstrip-based frequency reconfigurable antennas is their inability to maintain constant radiation characteristic over the different operating frequencies. For example, the radiation patterns in [3] are observed to be different when operating at low and high frequencies. To avoid this, other literature [2, 27–29] implemented more complicated DC biasing circuitries to achieve frequency reconfigurability. The losses incurred from the additional RF PIN or varactor diodes and the required lumped elements affects their final performance while increasing costs.

In this work, a frequency-reconfigurable circular patch antenna with dual-slot DGS is designed. First a large DGS is implemented to miniaturize the antenna. Then, three varactor diodes are placed across a small on the ground plane, with a simple biasing circuit for ease of fabrication. A T-slot is implemented on the circular patch to fine tune the lower operating frequency range of the antenna. The proposed antenna initially adopts the design concept based on a circular monopole antenna with slots [30–32] widely used in designing the UWB antennas with band notches. A simple DC biasing circuitry is used for this work. The proposed antenna achieved better average gain, whereas dipole-like patterns at all frequency bands are maintained by introducing a narrow slot to locate the varactor diodes. The fabricated antenna is capable of tuning over a large bandwidth (1.91 GHz to 2.77 GHz) with a tuning ratio of 1.5:1, which is an attractive feature in cognitive radio (CR) application. To the best of our knowledge, this work introduces a systematic and pioneering method on designing a frequency reconfigurable antenna with stable dipole-like radiation patterns at all operating frequencies. Moreover, the proposed design also featured a low gain fluctuation of 1.6 dB, and reduced complexity by using only three varactors in a compact structure. This manuscript is organized as follows. First, the three main design stages of the antenna and reconfiguration method is presented in the next section. This is followed by the details of the proposed antenna, simulations and measurement results in section III, including its performance comparison against

similar work available in literature. Finally, Section IV concludes this work.

## 2. Design of Antenna and Reconfiguration

### A. Circular Patch with dual-slot DGS

One important feature of reconfigurable antennas is to enable efficient tuning of the targeted parameter, while simultaneously maintaining the characteristics of other performance parameters [1, 20]. This is especially evident in the variation of the radiation patterns when designing frequency-reconfigurable antennas [3]. The reconfiguration to higher frequency may result in directional radiation patterns, whereas a quasi-omnidirectional radiation pattern can be generated at the lower frequencies. When all the RF switches are in ON state, the antenna operates at highest operating frequency. This is similar to the conventional microstrip patch antenna with the full ground plane. Hence, it generates a directional or quasi-omnidirectional radiation. In this work, the performance of antenna in terms of radiation pattern is achieved while the uniform radiation patterns are maintained. In Figure 1 the overall design procedure is illustrated. More details of the design procedure are provided as follows.

#### Stage A: Antenna Miniaturization

Firstly, a circular shaped patch is introduced in Stage A, and is fed using a microstrip line. Calculation of the patch size with this radius indicated that this antenna theoretically operates at 5.6 GHz. Nonetheless, a lower operating frequency of 2.8 GHz is noticed, and operation at this frequency is further optimized in the next stage to achieve a compact design.

#### Stage B: Integration of a Large Rectangular Slot DGS

This is followed by the integration of a DGS at ground plane, in Stage B. The slot DGS is optimized to ensure the antenna resonance is reduced to approximately 1.1 GHz, while maintaining a quasi-omnidirectional radiation pattern. The length of the DGS slot is important in shifting the resonant of the antenna towards 1.1 GHz. The slot length determines the resonant frequency of the antenna. The length is approximately  $\lambda_g/4$  where  $\lambda_g$  is the guided wavelength of the antenna with respect to resonant frequency. The DGS available is open (assuming the switches operating in the OFF state) will effectively enable the slot operating on the ground plane, hence generating a quasi-omni directional radiation pattern at 1.1 GHz. However, at ON condition, similar radiation characteristic is not attained. Note that the radiation pattern at this frequency is directive when the DGS is fully closed using an ideal an ideal ON condition of the PIN/varactor diode (assuming that switches will be implemented at this location based on [3]). This work specifically proposes a method to avoid such a scenario.

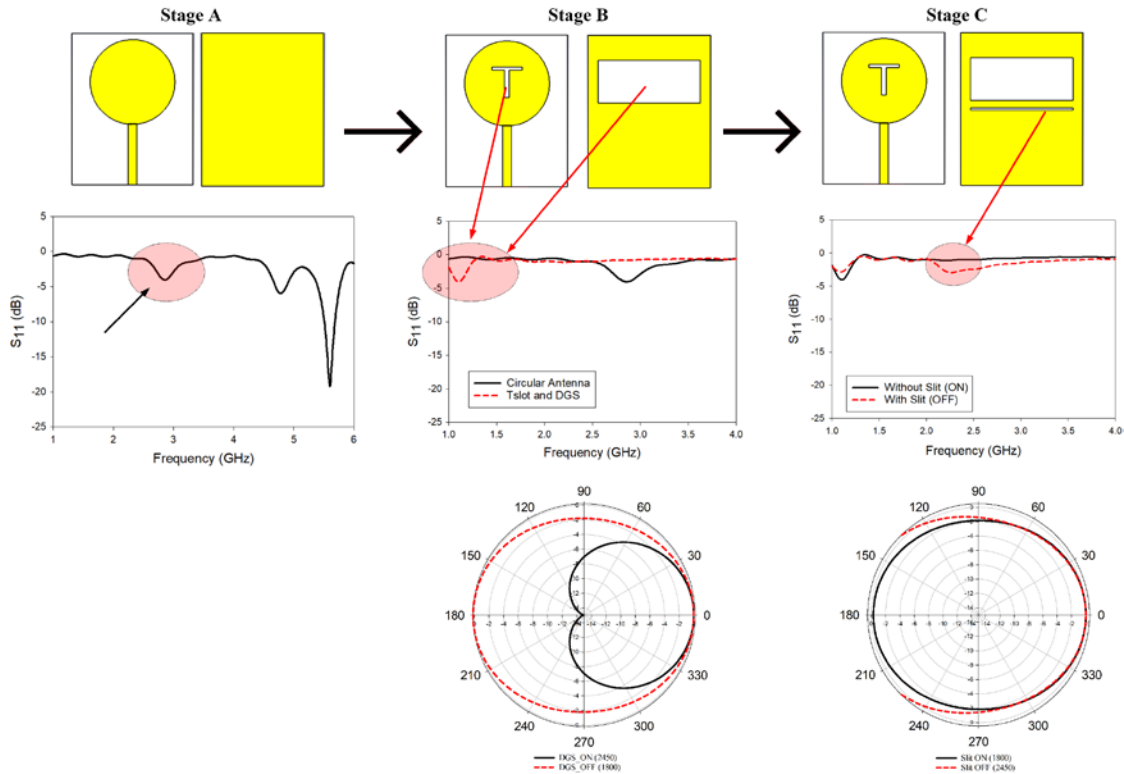


FIGURE 1. Design stages to achieve constant quasi-omni-directional radiation pattern.

### Stage C: Integration of a Narrow Slot DGS

If the switches are located at the original slot DGS at stage B, the tuning could be successful in terms of reflection coefficient ( $S_{11}$ ) but unable to maintain the radiation pattern. Therefore, a separate tuning location is dedicated. In that case, a new narrow slot is introduced for the tuning purpose. To overcome the radiation pattern inconsistency from the previous structure, a separate narrow slot is implemented on the ground plane. This is aimed to independently control the reconfiguration from the lower to the higher frequency while maintaining the quasi-omnidirectional radiation pattern. When the narrow slot is closed (with an ideal ON condition of the PIN/varactor diode), the antenna resonates near 2.3 GHz. Meanwhile, when this slot is open (with an ideal OFF condition of a diode), the antenna will resonate at 1.1 GHz. In other words, the best location for these RF switches will be across the narrow slot and not on the DGS. It can be seen that the radiation patterns for both cases are omni-directional. Note that, the optimizing the reflection coefficient result is not necessary at this stage, where optimization will be carried out during the DC biasing implementation where more structural modification will be required at the narrow slot to practically place the varactors. The optimized design is presented in next section, with the introduction of DC biasing circuit and modification on the narrow slot area to accommodate DC biasing lines.

### B. Optimized Frequency-Reconfigurable Antenna

The proposed antenna design and dimensions are presented in Figure 2. It is designed on FR4 substrate, which is 1.6 mm thick, with a dielectric constant of 4.5, and loss tangent of 0.019. The total size of the antenna ( $W \times L$ ) is 50.50 mm  $\times$  41.50 mm, including the biasing circuit. A feedline with a width and length ( $F_w \times F_l$ ) of 3 mm  $\times$  20.68 mm is designed to feed the patch antenna with a radius of  $R = 14.50$  mm. As depicted in Figure 2(a), a T-slot located on the patch antenna is dimensioned at  $S_1 = 10.00$  mm,  $S_2 = S_3 = 4.25$  mm,  $S_4 = S_6 = 1$  mm and  $S_5 = 9$  mm. The T-Slot is created to fine tune the lower operating frequency range. Other shaped slot also can be implemented to achieve similar purpose [33]. On the ground plane, a rectangular slot sized at ( $A \times B$ ) = 33.50 mm  $\times$  14.00 mm is placed exactly behind the radiator of the patch antenna. Another narrow slot is located on the ground plane to divide it into two parts. The upper ground length is  $G_1 = 24.10$  mm, whereas the lower part is  $G_2 = 24.60$  mm. Three parallel RF varactor diodes (SMV1232-079LF from *Skyworks, Inc.*) are placed across the slot. To locate these varactor diodes, six rectangular soldering pads are introduced onto the slot, with each sized at 2.00 mm  $\times$  0.50 mm. The photograph of the fabricated antenna prototype is shown in Figure 3. The distance between the three varactors is kept at  $E = F = 12.00$  mm. The width of the slot is  $C = 1.80$  mm, and other related dimensions of this slot are given as  $N = M = 5.75$  mm. A small

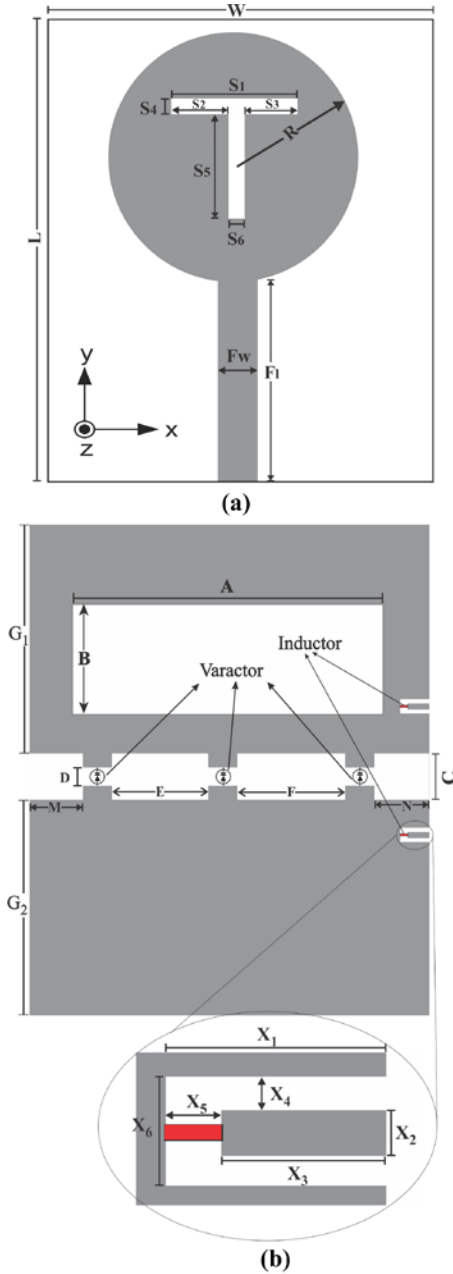


FIGURE 2. Geometry of the proposed antenna (a) front view and (b) back view.

gap is allocated for the varactor installation with a dimension of  $D = 0.80$  mm. Two small slots are used for biasing the RF varactor diode, as seen in Figure 2(b). The biasing slot is dimensioned at,  $X_1 = 2.00$  mm,  $X_2 = 0.40$  mm,  $X_3 = 1.50$  mm,  $X_4 = 0.30$  mm,  $X_5 = 0.50$  mm and  $X_6 = 1.00$  mm.

Figure 4(a) illustrates the full DC biasing circuitry, where two inductors,  $L_1 = L_2 = 27$  nH introduced to be biased simultaneously. These inductors are located on the ground plane on the antenna, as illustrated in Figure 2(b). They allow DC current flow to operate the varactor diodes while blocking the RF current leakages through the DC lines. Figure 4(b) shows the equivalent circuit of the varactor. The junction

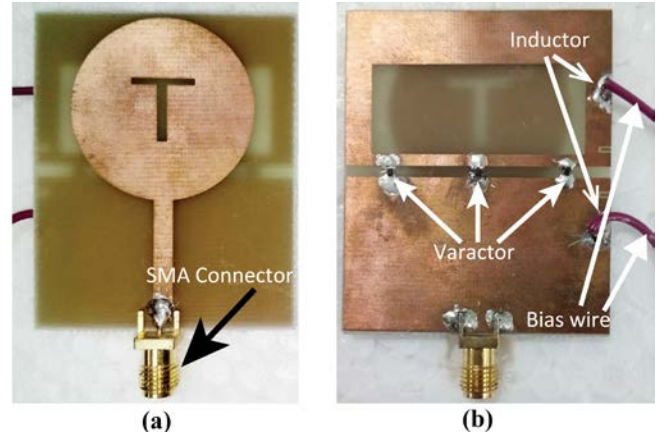


FIGURE 3. Photograph of the fabricated proposed antenna (a) front view, and (b) back view

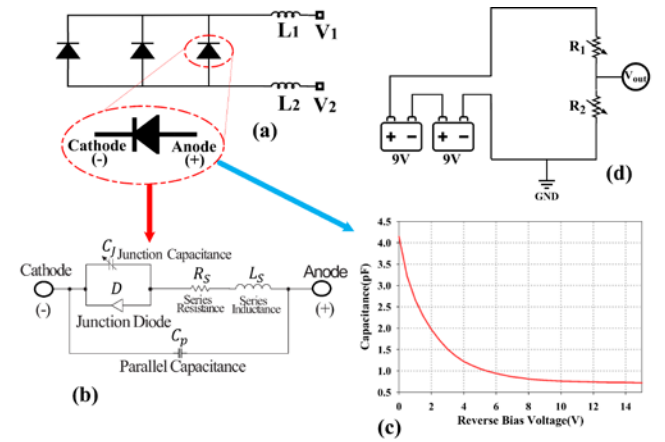


FIGURE 4. Illustration of DC biasing technique. (a) Full DC biasing circuitry (b) Simplified equivalent varactor circuit (c) The relation between the reverse bias and the capacitance (d) Designated biasing circuit diagram for the experiment.

capacitance of the varactor,  $C_j$ , is a function of the applied reverse DC voltage. The increase in the reverse bias voltage results in decreasing the capacitance of the varactor, and vice versa, as shown in Figure 4(c). The changes in capacitance of the varactor then tunes the operating frequency of the antenna. In this work, the capacitance values ranged from 1.51 pF to 0.72 pF, whereas the reverse bias voltages are between 3V and 13V (with a maximum allowable voltage of 15 V [34]). To practically implement this for experimental purposes, two 9V batteries are used with two resistors:  $R_1 = 5$  K $\Omega$  and  $R_2 = 25$  K $\Omega$ , as depicted in Figure 4(d). For the simulation purposes, touchstone blocks provided by the manufacturer [34] to ensure precision of results.

### 3 Results and Discussion

The  $S_{11}$  were acquired from the CST software, whereas the measured  $S_{11}$  were obtained from an Agilent E8362B Vector

Network Analyzer. The simulation results are presented in Figure 5, whereas the experimental  $S_{11}$  are shown in Figure 6. In all the operating frequency bands, the simulated and measured  $S_{11}$  is less than -14 dB. It can be noticed that there is minimal variation in terms of frequency bands between simulation and measurement results. Moreover, the measured reflection coefficient results in poor impedance matching compared to simulated result. These are caused by the additional resistance and loss introduced by the RF varactor diodes and biasing components such as DC blocking capacitors. The measured resonant frequencies are slightly shifted downwards for all operating bands, with an average shift of about 40 MHz. A more detailed performance of the proposed antenna is summarized in Table 1 for different reverse bias voltages. During  $S_{11}$  measurements, the prototype is biased using a Keysight E3631A DC power supply [35]. On the other hand, the circuit illustrated in Figure 4(d) was used for the DC biasing when measuring radiation patterns. This is due to the space limitation in the compact anechoic chamber. The measurement setup is illustrated in Figure 7(a). It can be noticed from Table 1 that there is a slight mismatch between simulation and measurement results. Despite this, the use of the varactor allowed slight retuning of the resonant frequency

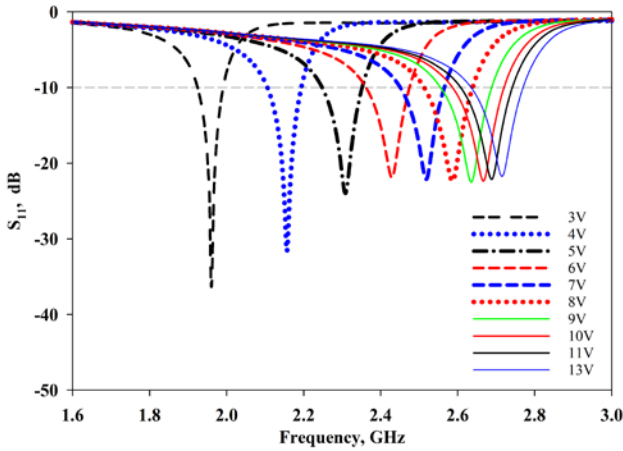


FIGURE 5. Simulated reflection coefficient,  $S_{11}$  results.

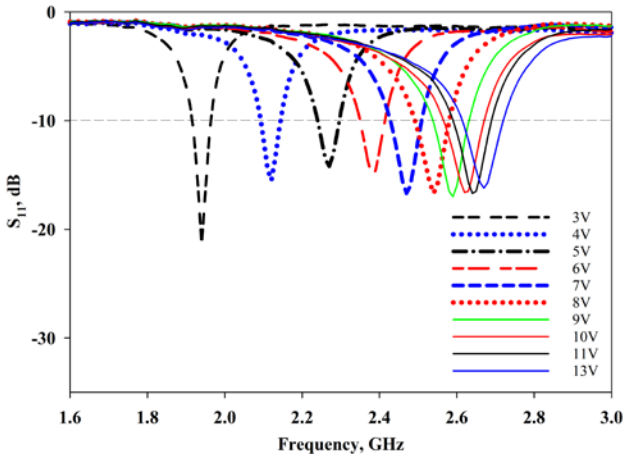


FIGURE 6. Measured reflection coefficient,  $S_{11}$  results.

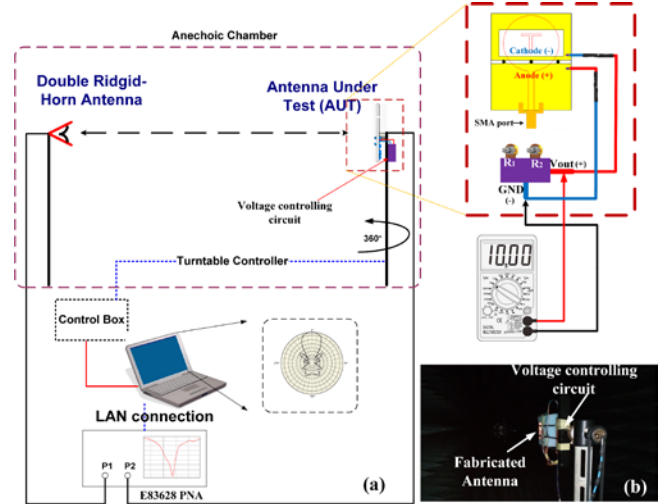


FIGURE 7. (a) Depiction of measurement setup. (b) Experimental setup in anechoic chamber.

TABLE 1. Simulated and Measured Resonant Frequency and Bandwidth.

Reverse bias voltage	Simulated resonant frequency	Measured resonant frequency	Simulated bandwidth	Measured bandwidth
3V	1.96 GHz	1.94 GHz	70 MHz	60 MHz
4V	2.15 GHz	2.12 GHz	100 MHz	60 MHz
5V	2.30 GHz	2.27 GHz	100 MHz	60 MHz
6V	2.43 GHz	2.39 GHz	120 MHz	70 MHz
7V	2.52 GHz	2.47 GHz	120 MHz	80 MHz
8V	2.58 GHz	2.54 GHz	130 MHz	90 MHz
9V	2.64 GHz	2.59 GHz	140 MHz	90 MHz
10V	2.67 GHz	2.62 GHz	140 MHz	110 MHz
11V	2.69 GHz	2.64 GHz	140 MHz	100 MHz
12V	2.70 GHz	2.66 GHz	140 MHz	100 MHz
13V	2.71 GHz	2.68 GHz	140 MHz	110 MHz

by slightly varying the applied reverse bias voltages. For instance, the measured resonant frequency of 1.96 GHz could be obtained with a reverse bias voltage of 3.1 V. The table also shows that the operational bandwidth for each resonant varies, where approximately average bandwidth of 85 MHz could be obtained. Although at one dedicated voltage a minimum bandwidth of 60 MHz is obtained, the use of varactor give freedom to tune the antenna if the bandwidth requirement is not achieved. For instance, the antenna tuning from 2 to 13 V will cover the whole bandwidth of 4G LTE mid-band frequencies from 1900 MHz to 2700 MHz.

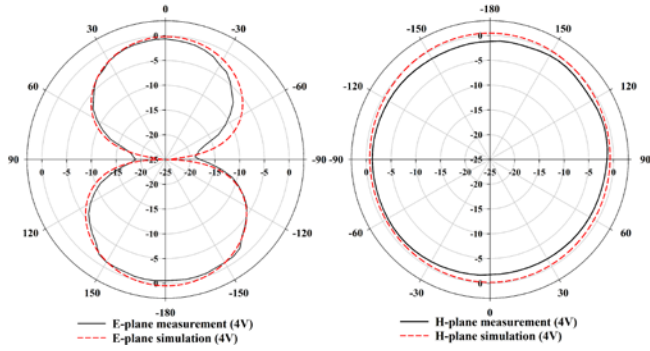


FIGURE 8. At 4V, simulated and measured radiation patterns. (a) E-plane and (b) H-plane.

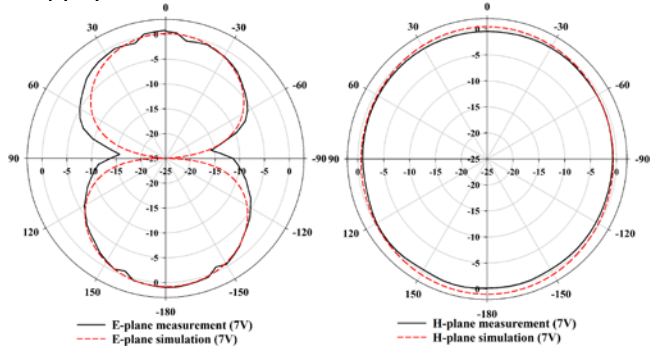


FIGURE 9. At 7V, simulated and measured radiation patterns. (a) E-plane and (b) H-plane.

Figure 7(b) exhibits the experimental setup in assessing radiation patterns. The simulated and measured radiation patterns of the proposed antenna for different applied reverse bias voltages are shown in Figure 8 (at 2.10 GHz), 9 (at 2.45 GHz) and 10 (at 2.65 GHz). Radiation patterns at all three frequencies and at both E-plane ( $xz$ -plane) and H-plane ( $yz$ -plane) are omnidirectional. The simulated and measured gain

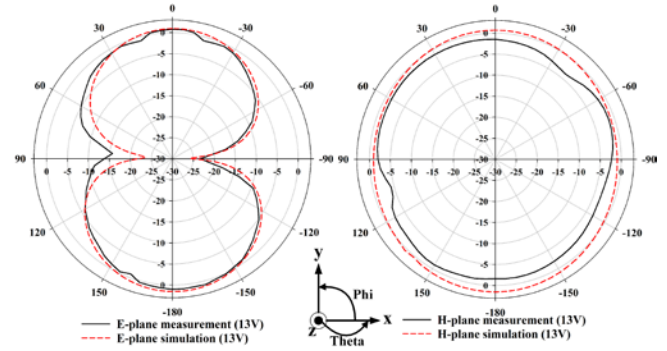


FIGURE 10. At 13V, simulated and measured radiation patterns. (a) E-plane and (b) H-plane.

over frequency is plotted throughout the frequency of operation is shown in Figure 11. There is a slight difference between the measured and simulated gains. This is due to the simulations which does not account for the losses from the RF varactor diodes and the lumped elements. It is also clear that as with higher frequencies, the gain of the antenna also improved.

A comparison between the proposed work with several previous literature is provided in Table 2. Despite being similar in terms of size and bandwidth, the DC biasing circuitry with four varactor diodes in [36] is relatively more complex. Moreover, this DC biasing line is not designed on the antenna, which may further degrade the performance of the slot-type antenna. Furthermore, this design is also not experimentally validated. Radiation stability can also be observed in work [2, 27–29, 37]. Amongst them, only [29] and [2] have experimentally assessed their radiation patterns. It is seen that both designs have not offered omnidirectional radiation patterns, and the work in [2] achieved a minimum gain fluctuation of 1.8 dB. On the other hand, [26, 28, 37, 38]

TABLE 2. Comparison of the proposed antenna with previous literature.

Ref	Antenna type	Antenna size (width $\times$ height $\times$ thickness)	Reconfiguration technique	Frequency coverage, Tuning ratio and Gain	Radiation pattern type & stability	Continuous/discrete	DC biasing	
							No of PIN/varactor diodes	Lumped elements
[36]	Slot antenna	$0.6\lambda_g \times 0.5\lambda_g \times 0.02\lambda_g$	Placement of the varactor diode including biasing circuit on a slotted ground plane	1.83 – 2.76 GHz & 1.5:1 1.8 ~ 2.4 dB (simulated)	Omnidirectional (stable)	C	4 Varactor diodes	$2 \times 47$ nH RF choke inductor
[28]	Grid-slotted patch antenna	$0.84\lambda_g \times 0.84\lambda_g \times 0.02\lambda_g$	The grid-slotted patch is mounted on the top layer with two tunable varactors, the microstrip line is located in the middle of two substrates and the ground plane is on the bottom layer.	2.45-3.55 GHz & 1.4:1 4.2 ~8.5 dB	Unidirectional pattern (stable)	C	2 Varactor diodes	$6 \times 33$ nH RF choke inductor

[39]	Slot-loop antenna	$0.32\lambda_g \times 0.54\lambda_g \times 0.01\lambda_g$	Two varactors are placed at the end of the rectangular ring slot.	2.14-3.33 GHz & 1.6:1 1~2.4 dB (simulated)	Omnidirectional pattern (stable)	C	2 Varactor diodes	$1 \times 100$ pF Capacitance, $1 \times 27$ k $\Omega$ Resistor
[38]	Patch antenna	-	Varactors diodes are place into the slotted structure of the patch antenna.	1.92-2.1 GHz & 1.1:1 -5 ~ 2.1 dB	-	C	2 Varactor diodes	-
[37]	Ring patch microstrip antenna	$1.48\lambda_g \times 1.48\lambda_g \times 0.06\lambda_g$	Varactor diodes are mounted on a square ring patch antenna and the L-shaped probe are utilized in the same layer for exiting the patch.	3.46-3.83 GHz & 1.1:1 0.5~6.5 dB	-	C	2 Varactor diodes	$1 \times 10$ k $\Omega$ Resistor
[40]	Rectangular patch	$0.40\lambda_g \times 0.6\lambda_g \times 0.02\lambda_g$	Varactor diodes are place on the slotted ground plan of the antenna.	2-3.8 GHz & 1.9:1 3.1~6.5 dB	Bidirectional pattern & Unidirectional (not stable)	C	2 Varactor diodes	$4 \times 40$ pF Capacitance, $3 \times 40$ nH RF choke inductor
[26]	Rectangular microstrip patch antenna	$0.70\lambda_g \times 0.70\lambda_g \times 0.04\lambda_g$	Varactor diodes are place on the slotted ground plan of the antenna	4.65-6.18 GHz & 1.3:1 0.8~7.2 dB (simulated)	Bidirectional pattern & Unidirectional (not stable)	C	2 Varactor diodes	-
[29]	Square patch	$1.19\lambda_g \times 1.19\lambda_g \times 0.03\lambda_g$	Three groups of switchable shorting pins connected to the ground plane and four controllable sections linked to the edge of the patch by p-i-n diodes.	1.83-2.65 GHz & 1.4:1 6~7.8 dB	Unidirectional (stable)	D	16 PIN diodes	$12 \times 860$ pF Capacitance, $16 \times 22$ nH RF choke inductor
[2]	Slot antenna	$0.63\lambda_g \times 0.69\lambda_g \times 0.02\lambda_g$	Placement of the RF PIN diode into the slot on the ground plane	2.2 – 4.75 GHz & 2.2:1 ~1.8 dB	Bidirectional in all frequency bands (stable)	D	5 PIN diodes	$14 \times 100$ pF capacitance
[3]	Microstrip patch-slot	$0.62\lambda_g \times 0.62\lambda_g \times 0.04\lambda_g$	Slot on the patch antenna; Placement of the RF PIN diode on the slotted ground plane	1.98 - 3.59 GHz & 1.8:1 0.2~4.8 dB	Unidirectional and Omnidirectional (not stable)	D	5 PIN diodes	$16 \times 100$ pF capacitance
This work	Circular	$0.56\lambda_g \times 0.68\lambda_g \times 0.02\lambda_g$	Parallel placement of varactor diode on a slotted ground plane	1.91 – 2.77 GHz & 1.5:1 0.2~1.8 dB	Omnidirectional in all frequency bands (stable)	C	3 Varactor diodes	$2 \times 27$ nH RF choke inductor120

\* $\lambda_g$  is calculated at the lowest operation frequency of the antenna

are lower in terms of frequency coverage and tuning ratios. Despite featuring improved frequency coverage, tuning ratio and simple DC biasing circuitries, the work in [39] and [20] have also not been validated experimentally. Moreover, their DC biasing difficult to be implemented in practice. Finally, the work in [2] and [3] did not capitalize the full capability of the five PIN diodes. Only several combinations were utilized in these designs out of the 32 possible switching combinations, despite being relatively wider in bandwidth. Besides this, the proposed DC biasing circuitries are more complex. No RF chokes or inductors were used, thus making RF current leakages on the DC lines highly possible. Based on these comparisons, the proposed antenna featured several distinct

advantages – it is compact, can be easily tuned, integrates a simple DC biasing circuitry and is cost effective. The capability of this antenna to maintain the dipole-like radiation pattern with gain fluctuation of 1.6 dB is another important feature of this antenna. This antenna works in the 2100 MHz band at 4 V, and in the 2.45 GHz band at 7 V, and thus can be applied for 4G-LTE and Wi-Fi applications.

#### 4 Conclusion

A frequency reconfigurable patch antenna incorporated with RF varactor diodes with low design complexity is proposed in this work. This antenna is capable of continuous frequency

reconfiguration to distinct frequency bands between 1.91 GHz and 2.77 GHz with a frequency ratio of 1.5:1. Frequency reconfigurability is performed using a simple biasing network consisting of three parallel RF varactor diodes located on the slotted ground plane. Besides enabling antenna compactness and fabrication simplicity, the antenna can be simply tuned by reverse biasing the voltage of this biasing circuit. Simulated and measured reflection coefficients and radiation patterns agreed well, featuring consistent omnidirectional radiation patterns. Such antenna features can be potentially compatible with cognitive radio applications.

## 5 Declarations

### A. Funding

The author would like to acknowledge the support from the Short-Term Research Grant (Mentorship) under a grant number of 9001-00600 from the Universiti Malaysia Perlis.

### B. Conflicts of interest/Competing interests

No conflict of interest/Competing interests

### C. Availability of data and material

Not applicable

### D. Code availability

Not applicable

### E. Authors' contributions

Conceptual design: Kabir Hossain, Thennarasan Sabapathy, Muzammil Jusoh and Ping Jack Soh.

Investigation and Methodology: R. Badlishah Ahmad and Mohd Ilman Jais.

Supervision: Thennarasan Sabapathy and Muzammil Jusoh

Concept visualization: Kabir Hossain, Thennarasan Sabapathy and Qammer H. Abbasi

Writing and editing: Kabir Hossain, Ping Jack Soh and Thennarasan Sabapathy

## References

- Christodoulou, C. G., Tawk, Y., Lane, S. A., & Erwin, S. R. (2012). Reconfigurable antennas for wireless and space applications. *Proceedings of the IEEE*, *100*(7), 2250–2261. <https://doi.org/10.1109/JPROC.2012.2188249>
- Majid, H. A., Rahim, M. K. A., Hamid, M. R., & Ismail, M. F. (2012). A compact frequency-Reconfigurable narrowband microstrip slot antenna. *IEEE Antennas and Wireless Propagation Letters*, *11*, 616–619. <https://doi.org/10.1109/LAWP.2012.2202869>
- Majid, H. A., Abdul Rahim, M. K., Hamid, M. R., Murad, N. A., & Ismail, M. F. (2013). Frequency-Reconfigurable Microstrip Patch-Slot Antenna. *IEEE Antennas and Wireless Propagation Letters*, *12*, 218–220. <https://doi.org/10.1109/LAWP.2013.2245293>
- Costantine, J., Tawk, Y., Barbin, S. E., & Christodoulou, C. G. (2015). Reconfigurable antennas: Design and applications. *Proceedings of the IEEE*, *103*(3), 424–437. <https://doi.org/10.1109/JPROC.2015.2396000>
- Rajo-Iglesias, E., Tawk, Y., Costantine, J., & Christodoulou, C. G. (2014). Wireless corner: Cognitive-radio and antenna functionalities: A tutorial. *IEEE Antennas and Propagation Magazine*, *56*(1), 231–243. <https://doi.org/10.1109/MAP.2014.6821791>
- Manjunatha, K. H., & Mehta, S. (2016). Reconfigurable communicating patch antenna for cognitive radio applications. In *2016 International Conference on Control, Instrumentation, Communication and Computational Technologies (ICCICCT)* (pp. 461–465). IEEE. <https://doi.org/10.1109/ICCICCT.2016.7987994>
- Salleh, S. M., Jusoh, M., Ismail, A. H., Kamarudin, M. R., Nobles, P., Rahim, M. K. A., ... Soh, P. J. (2017). Textile Antenna with Simultaneous Frequency and Polarization Reconfiguration for WBAN. *IEEE Access*, *6*(c), 7350–7358. <https://doi.org/10.1109/ACCESS.2017.2787018>
- Hossain, K., Sabapathy, T., Jusoh, M., Soh, P. J., Osman, M. N., Yasin, M. N. M., ... Podilchak, S. K. (2020). Pattern-Reconfigurable PCB-based Phased Array for WLAN Applications. In *2020 9th Asia-Pacific Conference on Antennas and Propagation (APCAP)* (pp. 1–2). Xiamen, China: IEEE. <https://doi.org/10.1109/APCAP50217.2020.9246130>
- Boufrioua, A. (2020). Frequency Reconfigurable Antenna Designs Using PIN Diode for Wireless Communication Applications. *Wireless Personal Communications*, *110*(4), 1879–1885. <https://doi.org/10.1007/s11277-019-06816-x>
- Behdad, N., & Sarabandi, K. (2006). A Varactor-Tuned Dual-Band Slot Antenna. *IEEE Transactions on Antennas and Propagation*, *54*(2), 401–408. <https://doi.org/10.1109/TAP.2005.863373>
- Jeong, W.-S., Lee, S.-Y., Lim, W.-G., Lim, H., & Yu, J.-W. (2008). Tunable Band-notched Ultra Wideband (UWB) Planar Monopole Antennas Using Varactor. In *2008 38th European Microwave Conference* (pp. 266–268). IEEE. <https://doi.org/10.1109/EUMC.2008.4751439>
- Oh, S.-S. S., Jung, Y.-B. B., Ju, Y.-R. R., & Park, H.-D. D. (2010). Frequency-tunable open-ring microstrip antenna using varactor. In *2010 International Conference on Electromagnetics in Advanced Applications* (pp. 624–626). IEEE. <https://doi.org/10.1109/ICEAA.2010.5652325>
- White, C. R., & Rebeiz, G. M. (2009). Single- and dual-polarized tunable slot-ring antennas. *IEEE Transactions on Antennas and Propagation*, *57*(1), 19–26. <https://doi.org/10.1109/TAP.2008.2009664>
- Nguyen-Trong, N., Piotrowski, A., & Fumeaux, C. (2017). A Frequency-Reconfigurable Dual-Band Low-Profile Monopolar Antenna. *IEEE Transactions on Antennas and Propagation*, *65*(7), 3336–3343. <https://doi.org/10.1109/TAP.2017.2702664>
- Punjala, S. S., Pissinou, N., & Makki, K. (2015). A Multiple Resonant Frequencies Circular Reconfigurable Antenna Investigated with Wireless Powering in a Concrete Block. *International Journal of Antennas and Propagation*, *2015*(2), 1–9. <https://doi.org/10.1155/2015/413642>
- Erdil, E., Topalli, K., Unlu, M., Civi, O. A., & Akin, T. (2007). Frequency Tunable Microstrip Patch Antenna Using RF MEMS Technology. *IEEE Transactions on Antennas and Propagation*, *55*(4), 1193–1196.

- <https://doi.org/10.1109/TAP.2007.893426>
17. Cetiner, B. A., Crusats, G. R., Jofre, L., & Biyikli, N. (2010). RF MEMS Integrated Frequency Reconfigurable Annular Slot Antenna. *IEEE Transactions on Antennas and Propagation*, 58(3), 626–632. <https://doi.org/10.1109/TAP.2009.2039300>
  18. Gautam, A. K., & Vishvakarma, B. R. (2007). Analysis of varactor loaded active microstrip antenna. *Microwave and Optical Technology Letters*, 49(2), 416–421. <https://doi.org/10.1002/mop.22154>
  19. Pandhare, R. A., & Abegaonkar, M. P. (2020). Inset-feed frequency reconfigurable compact e-shape patch with DGS. *Progress In Electromagnetics Research C*, 101(January), 119–132.
  20. Riaz, S., Zhao, X., & Geng, S. (2019). A compact frequency agile patch antenna with agile microstrip feedline. *2019 2nd International Conference on Computing, Mathematics and Engineering Technologies, iCoMET2019*, 1–4. <https://doi.org/10.1109/ICOMET.2019.8673512>
  21. Elftouh, H., Touhami, N. A., Aghoutane, M., Amrani, S. El, Tazon, A., & Boussouis, M. (2014). Miniaturized Microstrip Patch Antenna with Defected Ground Structure Reproduced courtesy of The Electromagnetics Academy Reproduced courtesy of The Electromagnetics Academy, 55(November), 25–33.
  22. Zhao, X., & Riaz, S. (2018). A Dual-Band Frequency Reconfigurable MIMO Patch-Slot Antenna Based on Reconfigurable Microstrip Feedline. *IEEE Access*, 6, 41450–41457. <https://doi.org/10.1109/ACCESS.2018.2858442>
  23. Riaz, S., Zhao, X., & Geng, S. (2020). A frequency reconfigurable MIMO antenna with agile feedline for cognitive radio applications. *International Journal of RF and Microwave Computer-Aided Engineering*, 30(3), 1–9. <https://doi.org/10.1002/mmce.22100>
  24. Hussain, R., Raza, A., Khan, M. U., Shammim, A., & Sharawi, M. S. (2019). Miniaturized frequency reconfigurable pentagonal MIMO slot antenna for interweave CR applications. *International Journal of RF and Microwave Computer-Aided Engineering*, 29(9), 1–12. <https://doi.org/10.1002/mmce.21811>
  25. Jenath Sathikbasha, M., & Nagarajan, V. (2020). Design of Multiband Frequency Reconfigurable Antenna with Defected Ground Structure for Wireless Applications. *Wireless Personal Communications*, 113(2), 867–892. <https://doi.org/10.1007/s11277-020-07256-8>
  26. Mahlaoui, Z., Antonino-Daviu, E., Ferrando-Bataller, M., Benchakroun, H., & Latif, A. (2017). Frequency reconfigurable patch antenna with defected ground structure using varactor diodes. *2017 11th European Conference on Antennas and Propagation, EUCAP 2017*, 2217–2220. <https://doi.org/10.23919/EuCAP.2017.7928358>
  27. Atallah, H. A., Abdel-Rahman, A. B., Yoshitomi, K., & Pokharel, R. K. (2016). Design of miniaturized reconfigurable slot antenna using varactor diodes for cognitive radio systems. In *Proceedings of the 2016 4th International Japan-Egypt Conference on Electronic, Communication and Computers, JEC-ECC 2016* (pp. 63–66). IEEE. <https://doi.org/10.1109/JEC-ECC.2016.7518968>
  28. Cai, Y. M., Li, K., Yin, Y., Gao, S., Hu, W., & Zhao, L. (2018). A low-profile frequency reconfigurable grid-slotted patch antenna. *IEEE Access*, 6, 36305–36312. <https://doi.org/10.1109/ACCESS.2018.2850926>
  29. Hu, J., & Hao, Z. C. (2018). Design of a frequency and polarization reconfigurable patch antenna with a stable gain. *IEEE Access*, 6, 68169–68175. <https://doi.org/10.1109/ACCESS.2018.2879498>
  30. Ibrahim, A. A., & Shubair, R. M. (2016). Reconfigurable band-notched UWB antenna for cognitive radio applications. *Mediterranean Microwave Symposium*, (c), 3–6. <https://doi.org/10.1109/MMS.2016.7803783>
  31. Jaglan, N., Gupta, S. D., & Srivastava, S. (2016). Notched UWB circular monopole antenna design using uni-planar EBG structures. *International Journal on Communications Antenna and Propagation*, 6(5), 266–273. <https://doi.org/10.15866/irecap.v6i5.9456>
  32. Jaglan, N., Gupta, S. D., Kanaujia, B. K., & Srivastava, S. (2018). Band notched UWB circular monopole antenna with inductance enhanced modified mushroom EBG structures. *Wireless Networks*, 24(2), 383–393. <https://doi.org/10.1007/s11276-016-1343-7>
  33. Yeo, J., & Lee, J. I. (2019). Slot-loaded microstrip patch sensor antenna for high-sensitivity permittivity characterization. *Electronics (Switzerland)*, 8(5). <https://doi.org/10.3390/electronics8050502>
  34. Skyworks. (n.d.). SMV1232 SERIES Hyperabrupt Junction Tuning Varactors. Retrieved September 15, 2020, from <https://www.skyworksinc.com/products/diodes/smv1232-series>
  35. Keysight Technoloiges. (2013). Keysight E3631A Triple Output DC Power Supply User's Guide.
  36. Avşar Aydın, E., & Kaya Keleş, M. (2019). UWB Rectangular Microstrip Patch Antenna Design in Matching Liquid and Evaluating the Classification Accuracy in Data Mining Using Random Forest Algorithm for Breast Cancer Detection with Microwave. *Journal of Electrical Engineering and Technology*, 14(5), 2127–2136. <https://doi.org/10.1007/s42835-019-00205-x>
  37. Tateno, H., Saito, S., & Kimura, Y. (2016). A frequency-tunable varactor-loaded single-layer ring microstrip antenna with a bias circuit on the backside of the ground plane. *2016 IEEE Antennas and Propagation Society International Symposium, APSURSI 2016 - Proceedings*, 829–830. <https://doi.org/10.1109/APS.2016.7696123>
  38. Sam, W. Y., & Zakaria, Z. (2017). The investigation of the varactor diode as tuning element on reconfigurable antenna. *APCAP 2016 - 2016 IEEE 5th Asia-Pacific Conference on Antennas and Propagation, Conference Proceedings*, 13–14. <https://doi.org/10.1109/APCAP.2016.7843076>
  39. Cheung, S. W., Cao, Y. F., & Yuk, T. I. (2015). Compact frequency reconfigurable slot antenna with continuous tuning range for cognitive radios. *2015 9th European Conference on Antennas and Propagation, EuCAP 2015*, 1–4.
  40. Mahlaoui, Z., Antonino-Daviu, E., Latif, A., & Ferrando-Bataller, M. (2019). Design of a dual-band frequency reconfigurable patch antenna based on characteristic modes. *International Journal of Antennas and Propagation*, 2019. <https://doi.org/10.1155/2019/4512532>